

---

# Changes in circulating small non-coding RNAs after castration in a cohort of prostate cancer patients

---

---

Received: 2 September 2025

---

Accepted: 29 January 2026

---

Published online: 03 February 2026

---

Cite this article as: Main A.M.,  
Sørensen L.H., Winge S.B. *et al.* Changes in circulating small non-coding RNAs after castration in a cohort of prostate cancer patients. *Sci Rep* (2026). <https://doi.org/10.1038/s41598-026-38334-9>

**Ailsa Maria Main, Louise Holst Sørensen, Sofia Boeg Winge, Mikkel Fode, Jens Sønksen, Anders Juul, Peter Busch Østergren, Nina Mørup & Kristian Almstrup**

---

We are providing an unedited version of this manuscript to give early access to its findings. Before final publication, the manuscript will undergo further editing. Please note there may be errors present which affect the content, and all legal disclaimers apply.

If this paper is publishing under a Transparent Peer Review model then Peer Review reports will publish with the final article.

# **Changes in circulating small non-coding RNAs after castration in a cohort of prostate cancer patients**

Ailsa Maria Main<sup>1,2,3,\*</sup>, Louise Holst Sørensen<sup>1,3</sup>, Sofia Boeg Winge<sup>1,3</sup>, Mikkel Fode<sup>4,5</sup>,  
Jens Sønksen<sup>4,5</sup>, Anders Juul<sup>1,3,5</sup>, Peter Busch Østergren<sup>4,5</sup>, Nina Mørup<sup>1,3</sup>, Kristian  
Almstrup<sup>1,2,3,\*</sup>

<sup>1</sup> Department of Growth and Reproduction, Copenhagen University Hospital - Rigshospitalet, Blegdamsvej 9, DK-2100, Copenhagen, Denmark

<sup>2</sup> Department of Cellular and Molecular Medicine, Faculty of Health and Medical Sciences, University of Copenhagen, Denmark

<sup>3</sup> International Center for Research and Research Training in Endocrine Disruption of Male Reproduction and Child Health, Denmark

<sup>4</sup> Department of Urology, Copenhagen University Hospital – Herlev and Gentofte, Herlev, Denmark

<sup>5</sup>Department of Clinical Medicine, University of Copenhagen, Denmark

## **\*Corresponding authors:**

Kristian Almstrup, [kristian.almstrup@regionh.dk](mailto:kristian.almstrup@regionh.dk)

Ailsa Maria Main, [ailsa.maria.main.02@regionh.dk](mailto:ailsa.maria.main.02@regionh.dk)

**Reprint requests should be addressed to:** Kristian Almstrup Department of Growth and Reproduction, Copenhagen University Hospital - Rigshospitalet, Blegdamsvej 9, DK-2100, Copenhagen, Denmark

**Key words:** small RNA sequencing, castration, endocrine biomarkers, testis.

## Abstract

Small non-coding RNAs (sncRNAs) can be found in circulation and may carry endocrine signals. Here, we analyse circulating sncRNAs before and after castration to identify sncRNAs that potentially could convey endocrine signals from the testis.

In a previous randomized clinical trial, men with advanced prostate cancer (n=57) were treated by either subcapsular orchiectomy (O-arm, n=28) or GnRH-analogue (G-arm, n=29). Blood samples were obtained at baseline (W0) and at 12 (W12) and 24 weeks (W24) post-intervention. Small non-coding RNAs from 169 longitudinally paired serum samples were sequenced using the RealSeq-Biofluids Small RNA kit.

A joint analysis of sncRNA reads at W12 and W24 compared to W0 identified 81 and 175 circulating sncRNAs present at significantly (FDR<0.05) different levels in the O-arm and G-arm, respectively. Most sncRNAs were found at lower levels after treatment (n=67 (83%) and n=150 (86%) in the O- and G-arm, respectively). The most prevalent type of sncRNA was piRNAs contributing to 44% (n=36 piRNAs) in the O-arm and 58% (n=101 piRNAs) in the G-arm. When the two treatment arms were analysed together, 16 sncRNAs were found to be consistently altered after castration. Of these sncRNAs, 8 were piRNAs and 4 have previously been reported in the testis, indicating a likely testicular origin. Using RT-qPCR and small RNA *in situ* hybridisation, we validated a testicular expression of miR-153 and SNORD38A.

In conclusion, the circulating sncRNA profiles are altered after castration and with a substantial loss of piRNAs indicating lost secretion of testicular sncRNAs. However, we cannot deduce if these circulating piRNAs mediate an endocrine signal.

# Introduction

Small non-coding RNAs (sncRNAs) are non-coding RNAs with a length shorter than 200 bp [1], and represent a very diverse group of RNAs, which are further sub grouped according to their size and putative functions. MicroRNAs (miRNAs) are the most well-described subgroup of sncRNAs and are involved in both suppression [2] and activation of gene expression [3, 4]. Besides the miRNAs, additional subgroups of sncRNAs include PIWI-interacting RNAs (piRNAs), tRNA-fragments (tRFs), small nucleolar RNAs (snoRNAs), and small nuclear RNAs (snRNAs). piRNAs are the largest group of sncRNAs and are mainly found in germ cells and appear to be essential for human spermatogenesis [5-7].

Albeit sncRNAs primarily exert their function intracellularly, some are also actively secreted to the extracellular environment [8]. Secretion can be mediated via small extracellular vesicles called exosomes [8], which is a tightly regulated process [8-10]. Exosomes are secreted by almost all cell types and enables delivery of e.g., sncRNAs to facilitate cell-to-cell communication [9]. Exosomes present proteins on their membrane which enables engulfment by specific recipient cells in which the sncRNAs can affect post-transcriptional regulation [11-13]. However, many sncRNAs found in circulation are also found outside of exosomes and protected from degradation by binding to proteins like AGO2 and lipoproteins [14, 15]. Hence, due to the stability in circulation, sncRNAs found in circulation can serve as a proxy for conditions in different tissues [9, 16]. Consequently, sncRNAs found in circulation has rapidly gained attention as valuable biomarkers of various pathological and physiological conditions [9]. Examples include circulating miR-371a as a highly accurate biomarker of testicular cancer [17], miR-1, miR-133, and miR-499 as biomarkers for myocardial infarction and heart failure [18] as well as

miR-375 and miR-126, which can be used in the diagnosis and management of diabetes [19].

Circulating sncRNAs have also been described as biomarkers of reproductive endocrinology. In rodents, miR-30b, miR-155, and miR-200b cause hypothalamic downregulation of GnRH blockers *MKRN3*, *CEBPB*, and *ZEB1*, respectively, which are crucial for the initiation of the GnRH pulse generator at the onset of puberty [20, 21]. In humans, miR-30b increase in circulation in boys treated for delayed puberty [22] and both miR-30b and miR-155 increase in circulation as puberty progresses in boys [23]. In addition, during GnRH stimulation tests, several piRNAs and the snoRNA, SNORD5, increase in circulation in boys who responded to GnRH with an increase in testosterone compared with boys where testosterone did not increase [24]. Furthermore, the levels of several circulating sncRNAs change as a consequence of both menopause and the use of hormone replacement therapy [25, 26]. However, the importance of circulating sncRNAs in reproductive endocrinology and to what extent sncRNAs mediate endocrine regulation is currently inadequately described.

Here, we take an exploratory approach to explore how circulating levels of sncRNAs change when an important reproductive endocrine tissue, the testis, is surgically removed or medically inactivated. We hypothesise that the profile of circulating sncRNAs change substantially when an endocrine organ is removed and present data from sequencing of circulating sncRNAs in a longitudinal cohort of patients with prostate cancer who were treated with either triptorelin (a GnRH agonist) or subcapsular orchietomy.

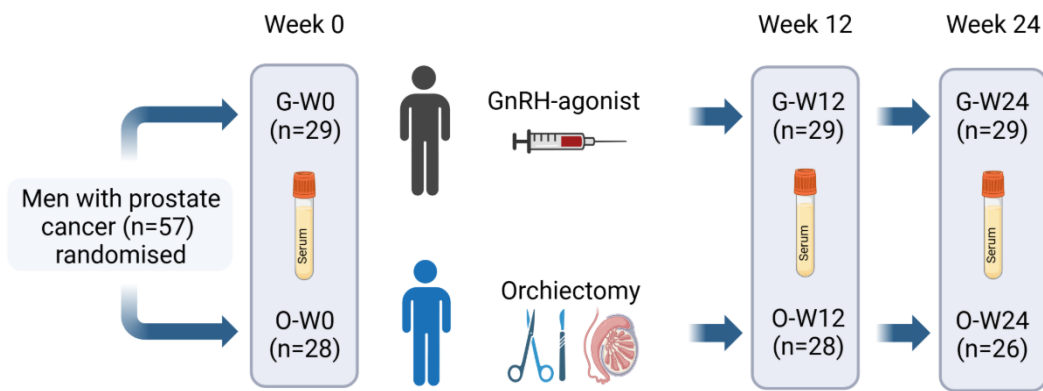
## Methods and materials

### Study participants

The participants in this study stem from a previous two-armed randomized trial conducted from 2013 to 2015 [27]. The trial evaluated the effect of 22.5 mg of the GnRH-agonist triptorelin (24-week depot injection) vs. subcapsular orchiectomy on metabolic changes and serum testosterone levels with the main objective to investigate differences in effect on body composition, glucose- and lipid metabolism and bone density. Men under 90 years of age with an Eastern Cooperative Oncology Group performance status (a tool used to measure the disease impact on a patient's daily living abilities (self-care, daily activity, and physical ability) [28])  $\leq 2$ , a confirmed diagnosis of prostate cancer without curative treatment options, and an indication for receiving androgen deprivation therapy were eligible for randomization. Exclusion criteria were prior androgen therapy, pharmacological treatment for osteoporosis, diabetes mellitus, and conditions (e.g., haemophilia) that substantially increased the risk of surgery (as decided by the treating physician). Participants allocated to the triptorelin arm were treated with the antiandrogen bicalutamide 50 mg daily for 30 days upon the first injection. Otherwise, the participants received no other treatments during the trial that could interfere with the gonadal axis [27]. A total of 57 participants were included in the cohort and randomised to castration either by the GnRH-agonist (G-arm, n=29) or by bilateral subcapsular orchiectomy (O-arm, n=28). Participants were evaluated at baseline prior to treatment and at 12, 24 and 48 weeks after the first injection or surgery, respectively. Venous blood samples for hormonal measurements were all collected between 8 and 9 a.m. All participants fasted for a minimum of 8 hours prior to each visit. Serum samples were stored at -80°C

[27]. For the current study, we included blood samples collected at 0 (W0), 12 (W12), and 24 (W24) weeks (Figure 1).

[Figure 1]



Serum samples were obtained before intervention at baseline week 0 (W0) and after intervention at week 12 (W12) and 24 (W24). The participants in the two treatment arms did not differ significantly in age, body mass index, or baseline testosterone levels, or Eastern Cooperative Oncology Group (ECOG) Performance Status Scale (Table 1). They also did not differ significantly in clinical tumour stage or Gleason staging as previously reported [29]. The cohort participants were on average between ECOG level 0 and 1; an ECOG of 0 means the patient is fully active with no performance restrictions, an ECOG of 1 classifies the patient as being restricted in terms of strenuous physical activity only but still fully ambulatory, and an ECOG of 2 states that the patient is ambulatory and capable of selfcare but unable to carry out any work activities. Data on changes in hormones, metabolic parameters, quality of life, and sexual function in this cohort have been published before [27, 29-31]. In total, 169 longitudinally paired serum samples collected at W0 (n=57) before intervention, and at W12 (n=57) and W24 (n=55) after intervention (Figure 1), were used in this study.

[Table 1]

**Table 1: Study population characteristics at baseline.** BMI = Body Mass Index, ECOG = Eastern Cooperative Oncology Group (ECOG) Performance Status Scale. Values are mean (SD) for age, BMI, and testosterone levels. ECOG values are n (%).

	O-arm	G-arm	p-value
<b>Individuals (n)</b>	28	29	-
<b>Treatment</b>	Subcapsular orchectomy	GnRH-analogue (Triptorelin)	
<b>Age</b>	72.1 (8.8)	74.8 (5.8)	0.18
<b>BMI</b>	27.0 (4.8)	27.6 (3.5)	0.60
<b>Testosterone (nmol/L)</b>	15.1 (6.5)	13.0 (6.3)	0.23
<b>ECOG n (%)</b>			
0	16 (57)	20 (69)	-
1	11 (39)	7 (24)	-
2	1 (4)	2 (7)	-

## RNA isolation, library preparation, and sequencing

RNA was extracted from 200 µL serum samples using the Quick-cfRNA Serum & Plasma Kit (Zymo Research, CA, USA, Cat No. R1059) according to the Manufacturer's instructions. Serum samples were stored at -80° Celsius and never thawed before analysis for this study. Due to the very small amounts of RNA in the samples, we were unable to run BioAnalyzer traces or perform similar RNA quality checks before generating libraries.

Sequencing libraries were prepared using the RealSeq-Biofluids library kit (RealSeq Biosciences, CA, USA, Cat. No. 600-00012 600-00048) according to the Manufacturer's instructions using 10 µL RNA elution as input and running 20 PCR cycles. The sequencing libraries were pooled to equal nanomolar concentrations

and then purified and size selected using a Pippin Prep (Sage Science, MA, USA). The library pools were subsequently profiled on a DNA Tapestation using the High Sensitivity DNA kit (Agilent, CA, USA, Cat. No. 5067-4626) and quantified with the high sensitivity kit on a dsDNA High Sensitivity Qubit (Thermo Fisher Scientific, MA, USA, Cat. No. Q32851). Pooled sequencing libraries were sequenced to a depth of 50M on a NextSeq 550 (Illumina, CA, USA, Cat. No. SY-415-1002) using 75 bp single-stranded reads.

## Bioinformatics analysis

Demultiplexed FASTQ files were trimmed using *Cutadapt* [32]. Adapter sequences were removed, and reads were filtered based on a minimum length of 15 bp. The trimmed reads were mapped to various databases sequentially using Bowtie 1.3.1 [33], ensuring that a read that had been mapped to one database did not map to others. The order of alignments was rRNA > tRNAs (with CCA tails) > other ncRNAs > cDNAs > genome. The following annotation databases were used: RNA Central (rRNA), GtRNAdb (tRNA), MirGeneDB (miRNA), piRBase (piRNA using the high confidence set), and Ensembl (other ncRNAs and cDNA). For multi-mapped reads, the best alignment was chosen and in the case of equally scoring alignments, the selection was random. Reads with no annotated features were labelled as "other." The average mapped reads per sample were 10,052,269 and the data from each sample were used to create an annotated read count matrix.

## Data analysis

The read count matrix was imported into R studio (version 2024.04.2+764 using R version 4.4.1) and analysed using the edgeR package [34]. Annotated sncRNAs ( $n = 107,216$ ) with less than 1 count per million in two samples were filtered out,

leaving 61,618 sncRNAs for analysis. Reads originating from long RNAs (types: antisense, lncRNA, protein-coding, rRNA, pre-mRNA) were excluded and the data were normalized to the library size. Potential outliers were identified by inspection of multidimensional scaling, principal component and contamination plots and five samples, O-W0-10, G-W24-1, G-W24-6, G-W24-5, and O-W24-41 were found to either group distant from all other samples ( $n = 3$ ) (Supplementary Figure 1a and 1b) or had high levels of contamination ( $n = 2$ ) (Supplementary Figure 1c) and were excluded from downstream analyses. Hence, in total 164 samples were included in the subsequent analysis. The distribution of samples across timepoints was as follows: In the O-arm 27 samples at W0, 28 samples at W12, and 25 samples at W24. In the G-arm there were 29 samples at W0, 29 samples at W12, and 26 samples at W24.

Generalised linear models were used to identify differentially expressed sncRNAs. Three different contrasts were considered for each arm: W0 vs. W12, W0 vs W24, and W0 vs W12+W24. A false discovery rate (FDR) q-value of 0.05 was used as a cut-off in identifying differentially expressed sncRNAs. To test for enrichment, a hypergeometric distribution was applied using the *phyper* function. The R package *EnhancedVolcano* [35] was used to draw volcano plots of the contrasts. The R packages *ggplot2* [36], *ggpubr* [37] were used to draw all other plots.

Several different online databases were queried to search for available information on the identified sncRNAs. For piRNAs, The Human Body Map 2.0 project track in Ensembl (Ensemble Release 113 – October 2024) [38] was used to gather information on RNAseq reads in the testis and piRBase v.3 [39] was used to search for previous findings in germ cells and potential target genes. miRNA tissue expression was based on information from the miRNA TissueAtlas 2025 [40] and for each miRNA, information on the top 5 target genes was based on the miRDB

target prediction database [41, 42]. For snoRNAs, the information on tissue expression was based on SnoDb version 2.0, Scott Group Bioinformatics [43]. GTEx (phs000424.v10.p2) [44] was used to gather information on tissue expression for all snRNAs.

## RT-qPCR

RT-qPCR was performed on tissues originating from testis samples (n=3), skin (n=1), prostate (n=1), and epididymis (n=1). Two different setups were used for cDNA synthesis and RT-qPCR based on the type of sncRNA interrogated. In both cases, total human RNA from six different commercially available RNA samples were used as input. RNA from testis tissue, epididymis, and skin was acquired from BioChain Institute Inc. (CA, USA; two different lots of Cat No. R1234260-50, R1234105-10-A703144, and R1234218-50, respectively). An additional RNA from testis tissue was acquired from Takara Bio Inc. (Japan, Cat No. 636533), and RNA from prostate tissue was acquired from Thermo Fisher Scientific (MA, USA, Cat No. Q50624).

To measure the expression of miR-153-1, 1 µg of RNA was reverse transcribed using the High-Capacity cDNA Reverse Transcription Kit (Thermo Fisher Scientific, MA, USA, Cat No. 4368814) according to the Manufacturer's instructions. Quantification was performed using the TaqMan™ Fast Advanced Master Mix, no UNG (Thermo Fisher Scientific, MA, USA, Cat No. A44360) with the TaqMan™ Pri-miRNA Assay (hsa-miR-153-1) (Thermo Fisher Scientific, MA, USA, Assay ID: Hs03303182\_pri, Cat No. A44360) and ACTB as housekeeping gene (Thermo Fisher Scientific, MA, USA, Assay ID: Hs01060665\_g1, Cat No. 4331182) according to the Manufacturer's instructions. The reaction was incubated in a thermal cycler

at 50 °C for 2 min, 95 °C for 20 sec followed by 40 cycles of 95 °C for 1 sec and 60 °C for 20 sec.

To quantify the levels of SNORD38A, 1 µg of RNA was reverse transcribed with AMV reverse transcriptase (Promega, Madison, WI, USA, Cat No. M5101) using a dT20 primer and random hexamers according to the manufacturer's instructions. Quantification was performed using the PowerUp™ SYBR™ Green Master Mix (Applied Biosystems, MA, USA, Cat No. A25741) and primers against SNORD38a (forward primer: TCTCGTGATGAAAAGTCTGTCC and reverse primer: GGCTCTCATCTCTCCCTTC) and RPS20 as housekeeping gene (forward primer: AACAAAGCCGCAACGTAAAATC and reverse primer: ACGATCCCACGTCTAGAAC) according to the Manufacturer's instructions. The samples were incubated in the thermal cycler at 95 °C for 15 min and 40 cycles of 95 °C for 15 sec and 62 °C for 1 min.

All samples were run in triplicates in a 96-well standard PCR plate on QuantStudio Pro 6 (Thermo Fisher Scientific, MA, USA). Relative expression was calculated using the  $2^{-\Delta\Delta CT}$  method with ACTB as an endogenous control. For testis, biological replicates (n=3) were available, whereas for skin, prostate, and epididymis the replicates are technical only.

## Small RNA *in situ* hybridisation

The testis tissue samples were excised from tumour-free periphery of orchiectomy specimens from two adult men with testicular germ cell tumours. Following surgical excision, the tissue was immediately fixed in 10% neutral-buffered formalin for at least 16 hours. The tissue was then dehydrated and embedded in paraffin. Small RNA *in situ* hybridisation experiments were performed on 4 µm sections mounted on SuperFrost PlusTM Slides (Thermo Fisher Scientific, MA, USA)

using the miRNAscope® 2.5 HD Detection Reagent - RED kit according to the Manufacturer's recommendations (Advanced Cell Diagnostics, CA, USA). Briefly, testicular tissue sections were dewaxed in xylene and washed in 100% ethanol followed by post-fixation in 10% neutral-buffered formalin. On the next morning, the slides were treated with hydrogen peroxide for 10 min. Target retrieval was performed for 15 min at 99 °C followed by treatment with protease III for 40 min at 40 °C. The slides were hybridized with Hs-SNORD38A-S1 (Advanced Cell Diagnostics, CA, USA, Cat No. 1807041-S1) for 2 hours at 40 °C followed by overnight incubation in 5X SSC (750 mM sodium chloride and 75 mM trisodium citrate, pH 7.0) buffer. On the next day, the slides were treated with a series of signal amplifications (with amplification round 5 for 40 min) and visualisation was performed using Fast Red. The sections were counterstained with Mayer's haematoxylin and dried before mounting with Vectamount® Permanent Mounting Medium (Vector Laboratories, CA, USA). The negative control probe (Cat No. 727881-S1) was run in parallel with the target probes and showed less than 5% positive cells. All slides were visualized using a NanoZoomer 2.0HT slide scanner (Hamamatsu Photonics, Japan).

## Ethics

The trial was conducted in accordance with the Declaration of Helsinki and the legal regulations in Denmark. Permission was obtained from the Danish Medicines Agency (EudraCT 2013-002553-29; registered on [www.clinicaltrialsregister.eu](http://www.clinicaltrialsregister.eu); <https://www.clinicaltrialsregister.eu/ctr-search/trial/2013-002553-29/results> with publication date 29 Nov 2021) and the Capital Regional Committee on Health Research Ethics in Denmark (H-2-2013-107 and H-16019637). A CONSORT

checklist is included as a supplementary file. All patients gave informed consent before inclusion.

ARTICLE IN PRESS

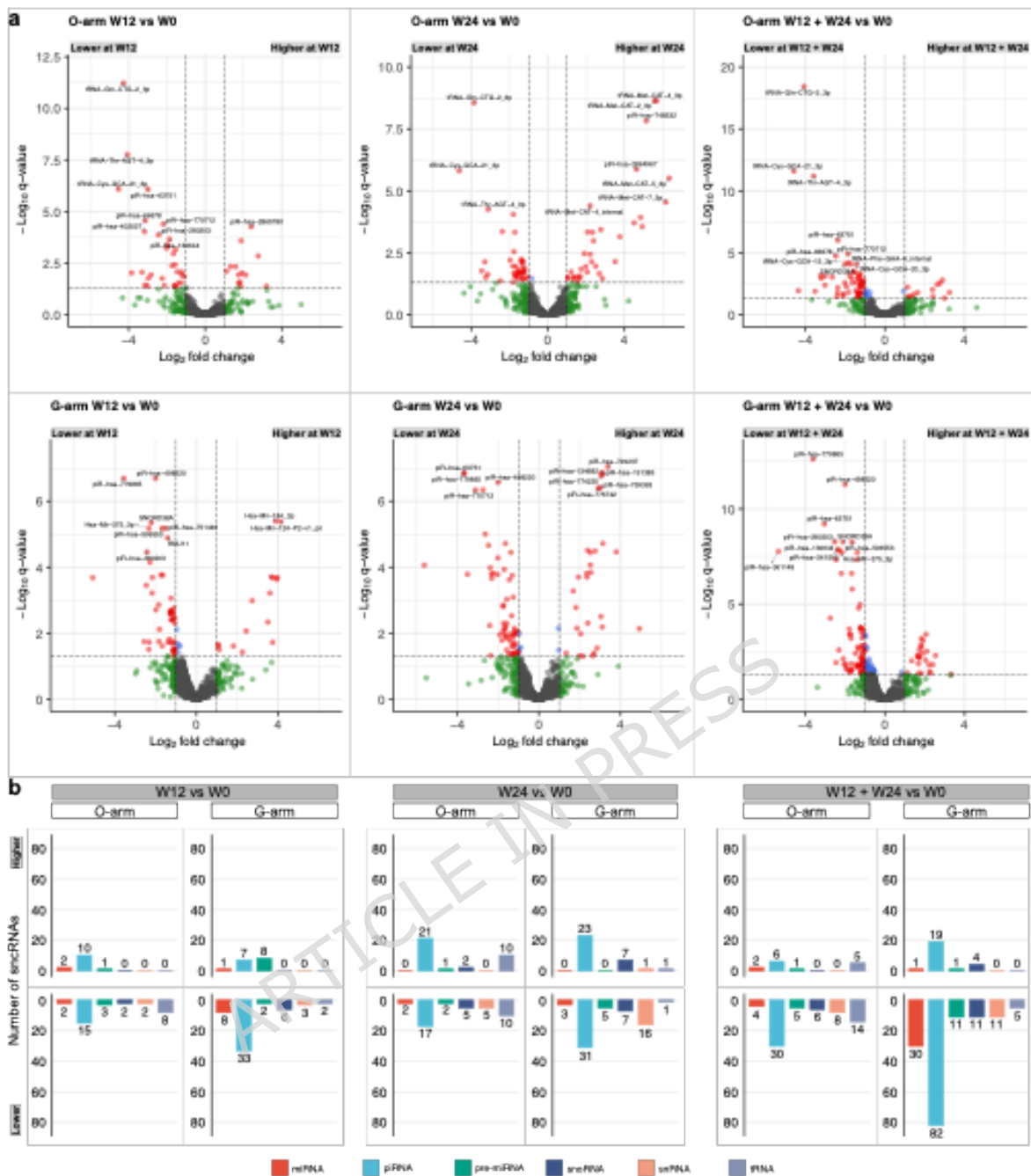
# Results

## Differentially present sncRNAs

We performed differential expression analysis on sncRNAs from the 164 serum samples, 84 in the G-arm and 80 in the O-arm.

In the O-arm, differential expression analysis using generalised linear models revealed 45 (13 at higher and 32 at lower levels) and 75 (34 at higher levels and 41 at lower levels) sncRNAs present in significantly different levels at W12 and W24, respectively, vs W0 (Figure 2a). A joint analysis of W12 + W24 vs W0 revealed 81 (14 at higher levels and 67 at lower levels) sncRNAs present at significantly different levels (Figure 2a).

[Figure 2]



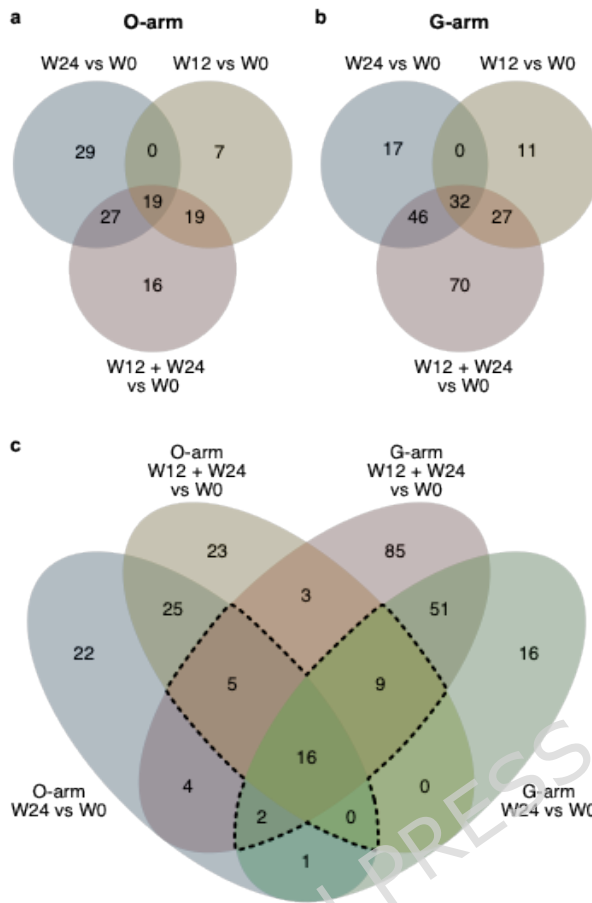
Similar observations were discovered in the G-arm, which revealed 70 (16 at higher and 54 at lower levels) and 95 (32 at higher and 63 at lower levels) sncRNAs present in significantly different levels at W12 and W24, respectively, vs W0 (Figure 2a). Joint analysis of W12 + W24 vs W0 revealed 175 (25 at higher levels and 150 at lower levels) sncRNAs present at significantly different levels (Figure 2a).

In both the O and G-arm, more sncRNAs were identified at W24 in comparison to W12 (75 vs 45 and 95 vs 70, O- and G-arm respectively) and most were found to be downregulated after intervention (W12+W24 vs W0; 67/81 (83%) and 150/175 (86%) in the O- and G-arm, respectively), indicating a gradual but pronounced loss of circulating sncRNAs after castration (Figure 2b). The most prevalent type of sncRNA identified to be differentially present after castration was piRNAs contributing to 44% (36 piRNAs,  $p=0.003$ ) in the O-arm and 58% (101 piRNAs,  $p=2.3e-16$ ) in the G-arm, indicating a gradual loss of sncRNAs from the testis. All significant sncRNAs identified are listed in Supplementary File 1.

## Overlapping sncRNAs

To identify circulating sncRNAs that consistently show alterations after both types of intervention and time points, we constructed Venn diagrams to display overlapping sncRNAs. In the O-arm (Figure 3a) the number of differentially present sncRNAs across all three contrasts was 19 out of 117 (16%) sncRNAs and in the G-arm it was 32 out of 203 (16%) (Figure 3b). When the two treatment arms were analysed together, 16 sncRNAs were found to be consistently altered after castration (Figure 3c).

[Figure 3]



These 16 sncRNAs are listed in Table 2 together with 16 other sncRNAs that were differentially altered in 3 of the 4 groups compared within each arm of the study (indicated by the dashed line in Figure 3c). We searched for available information on these sncRNAs, which revealed that out of the 32 sncRNAs listed in Table 2, 12 of the sncRNAs show reads from testis tissue according to the Human Body Map 2.0 project. Additionally, 20 piRNAs have been reported in germ cells according to piRBase and 9 other sncRNAs have been reported in the testis. Taken together, this indicates a likely testicular origin of most of the identified sncRNAs. However, we also noted 4 sncRNAs reported in the prostate.

For the piRNAs, piRBase revealed seven piRNAs potentially targeting *HSPA9* and *SNORD63*, six piRNAs potentially targeting *PLEKHA8P1* and/or ENSG00000286171 and two piRNAs potentially targeting *THAP8*. Three of these genes (*HSPA9*, *PLEKHA8P1*, and *THAP8*) show expression in the testis according to the GTEx portal.

For mature miRNAs, the top-5 potential target genes according to the target prediction database in miRDB are listed in Table 2.

**Table 2: Information on the 32 differentially expressed sncRNAs (dashed lines in Figure 3c).** The information in the table was obtained from various databases as listed in the Methods and Materials section.

	O-arm logFC (FDR)	G-arm logFC (FDR)	piRNAs		miRNAs, snRNAs and snoRNAs		Potential target genes
			Testis RNAseq reads	Reported in germ cells	Expression in testis and prostate		
<b>Intersecting all 4 group</b>							
piR-hsa-2864967	2.77 (0.0028)	1.71 (0.0132)	Yes	Yes	-	-	
piR-hsa-770712	-1.87 (1.2*10^-5)	-2.46 (4.7*10^-8)	Yes	Yes	-	PLEKHA8P1, ENSG00000286171	
piR-hsa-66678	-2.48 (1.8 *10^-5)	-2.75 (5.4*10^-5)	Yes	Yes	-	THAP8	
piR-hsa-63751	-2.36 (9.7*10^-7)	-3.05 (6.2*10^-10)	Yes	Yes	-	THAP8	
piR-hsa-741466	-1.19 (0.0018)	-1.2 (0.0003)	No	Yes	-	HSPA9, SNORD63	
piR-hsa-1242875	-1.13 0.0023)	-1.24 (0.0002)	No	Yes	-	HSPA9, SNORD63	
piR-hsa-1288242	-1.11 (0.0032)	-1.22 (0.0002)	No	Yes	-	HSPA9, SNORD63	
piR-hsa-1254147	-0.96 (0.024)	-1.12 (0.0034)	No	Yes	-	HSPA9, SNORD63	
Hsa-Mir-153-P2-pri	-1.68 (0.0011)	-1.28 (0.0075)	-	-	Testis and prostate	UNC5C, KCNQ4, SERTAD2, KLF5, HEY2	
Hsa-Mir-153-P1-pri	-1.78 (0.0007)	-1.19 (0.0077)	-	-	Testis and prostate	UNC5C, KCNQ4, SERTAD2, KLF5, HEY2	
tRNA-Gln-CTG-2_3p	-4.07 (3.7*10^-19)	-0.82 (0.023)	-	-	-	-	
RNU5B-1	-1.23 (0.00057)	-1.67 (2.4*10^-7)	-	-	Highest median expression in testis	-	
RNU11	-1.07 (0.0016)	-1.39 (2.0*10^-8)	-	-	-	-	
SNORD38A	-2 (8.3*10^-5)	-2.12 (5.4*10^-9)	-	-	Testis	-	
SNORD26	-1.29 (0.0015)	-1.14 (0.0017)	-	-	Testis	-	
SNORA2C	-1.07 (0.0059)	-1.22 (0.0002)	-	-	Testis	-	
<b>Intersecting 3 out of 4 groups</b>							
piR-hsa-130644	-1.51 (0.00035)	-2.3 (1.4*10^-8)	Yes	Yes	-	ENSG00000286171	
piR-hsa-774082	-1.37 (0.00091)	-1.71 (0.0006)	Yes	Yes	-	PLEKHA8P1, ENSG00000286171	
piR-hsa-368867	-1.24 (0.0044)	-1.79 (0.0002)	Yes	Yes	-	PLEKHA8P1, ENSG00000286171	
piR-hsa-102217	-1.95 (0.0052)	-2.05 (0.014)	Yes	Yes	-	-	
piR-hsa-147022	-1.21 (0.0058)	-1.73 (0.0004)	Yes	Yes	-	PLEKHA8P1, ENSG00000286171	
piR-hsa-280203	-1.46 (0.0105)	-2.53 (5.4*10^-9)	Yes	Yes	-	-	
piR-hsa-167536	-0.91(0.0114)	-1.06 (0.039)	Yes	Yes	-	PLEKHA8P1, ENSG00000286171	
SNORD14D	-1.39 (0.017)	-1.39 (0.017)	-	-	Testis	-	
piR-hsa-762831	-1.26 (0.035)	1.7 (0.0061)	Yes	Yes	-	-	

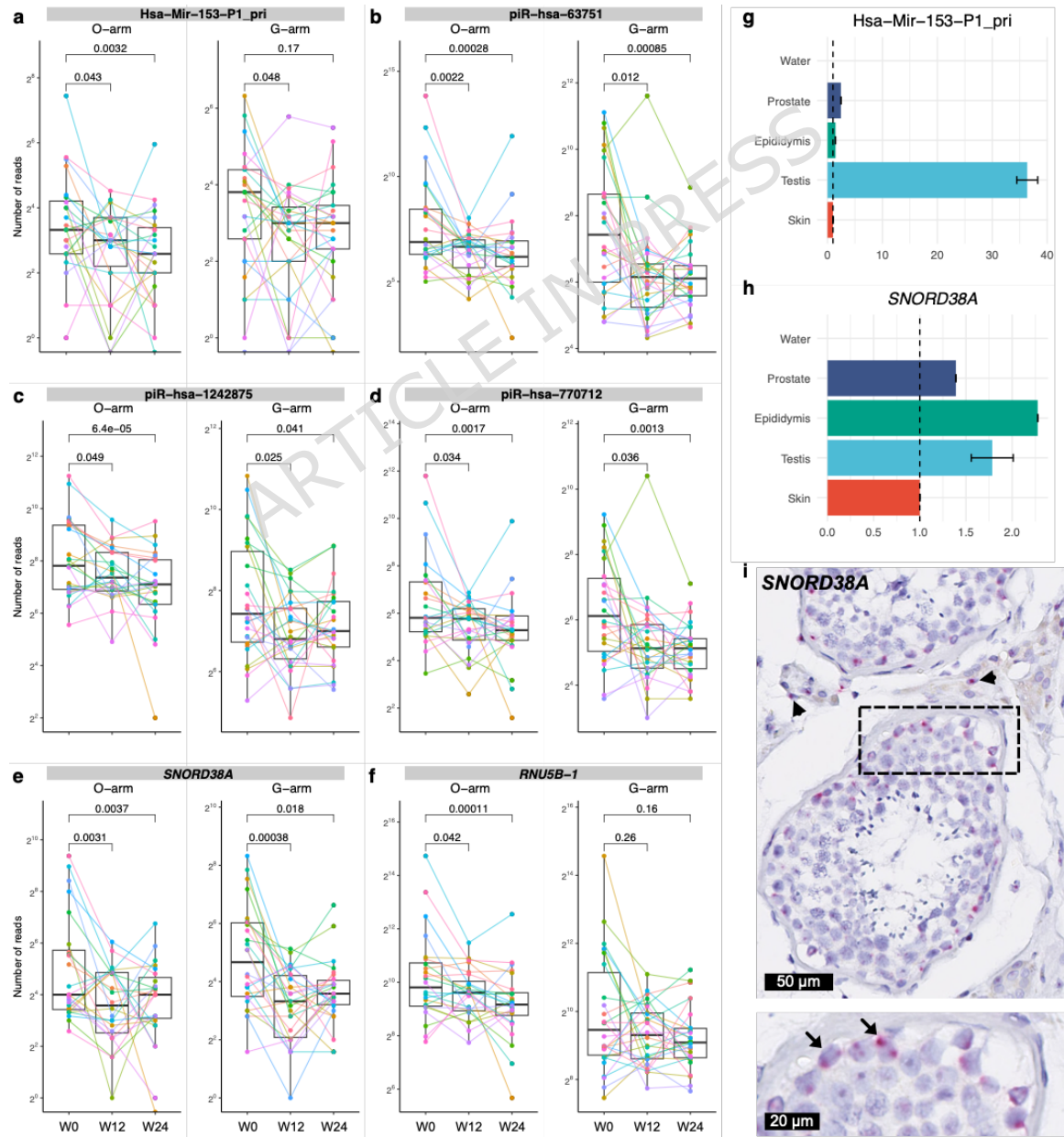
piR-hsa-1301393	-1.18 (0.0027)	-0.98 (0.012)	No	Yes	-	HSPA9, SNORD63
piR-hsa-736316	-1.09 (0.016)	-1.03 (0.024)	No	Yes	-	HSPA9, SNORD63
piR-hsa-777409	-0.94 (0.028)	-0.99 (0.015)	No	Yes		HSPA9, SNORD63
Hsa-Mir-184_3p	-1.25 (0.0042)	1.68 (0.043)	-	-	Testis and prostate	SETD9, NUS1, CES2, PLPP3, GNB1
tRNA-Thr-AGT-4_3p	3.59 (6.3*10^-12)	-0.98 (0.034)	-	-	-	-
piR-hsa-82907	2.50 (0.0109) (W24)	2.05 (0.0087)	No	Yes	-	SNHG1
Hsa-Mir-96-P2_pri	2.39 (0.001) (W24)	-1.15 (0.0015)	-	-	Testis and prostate	NEXMIF, ADCY6, PRTG, SPIN1, FRS2

The information in the table was obtained from various databases as listed in the Methods and Materials section.

## Individual alterations and testicular expression

Longitudinal changes in levels of six of the best separating sncRNAs from Table 2 are shown in Figure 4a-f. The longitudinal changes in the remaining sncRNAs with 4 interactions from Table 2 are shown in Supplementary Figure 2. The paired analysis confirmed significantly lower levels post-intervention of the selected sncRNAs, except RNU5B-1 in the G arm (Figure 4f).

[Figure 4]



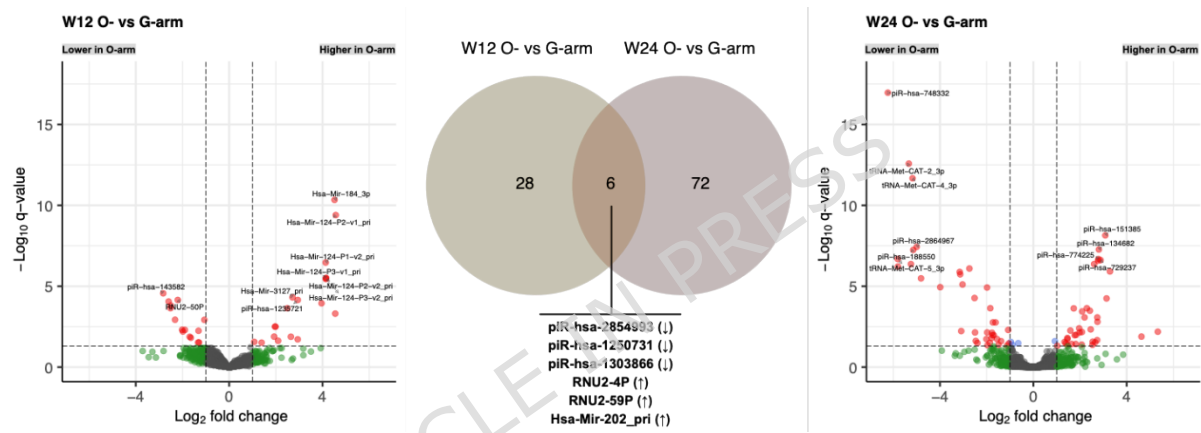
We chose to validate the possible testicular origin of miR-153-1 and SNORD38A by RT-qPCR and *in situ* hybridisation as they were two of the sncRNAs that showed a prominent and significant alteration. Furthermore, they had previously been found to be expressed in testis tissue (Table 2). The RT-qPCR showed, that when compared to expression in skin, the level of miR-153-P1\_pri appeared to be enriched in the testis (Figure 4g). In contrast, *SNORD38A* appeared more ubiquitously expressed showing similar expression levels across the four organs (Figure 4h). However, miR-153-P1\_pri was expressed at much lower levels in skin compared to *SNORD38A*, which makes direct comparison of expression levels difficult (data not shown). Small RNA *in situ* hybridisation confirmed a prominent expression of *SNORD38A* in testis tissue, where expression was primarily observed in spermatogonia, but also at lower levels in Leydig and peritubular cells (Figure 4i). Bearing in mind that the RT-qPCR and *in situ* hybridisation do not allow for a broader generalisation, the analyses could indicate that the lower circulating levels of miR-153-1 and *SNORD38A* after the intervention is due to the loss of the testicular secretion into circulation.

## Differences between the two interventions

Both interventions aim to decrease testicular testosterone production but accomplish this in distinctly different ways. We analysed if any sncRNAs were differentially present in circulation according to the type of intervention. Analysis between patients in the two treatment arms revealed 34 and 78 sncRNAs present in significantly different levels at W12 and W24, respectively (Figure 5). The sncRNA identified at each time point could reflect different types of variation (treatment response, side-effects etc.) between the two treatment groups, and only six sncRNAs were consistently identified at both W12 and W24 (Figure 5). Of these six sncRNAs, three were piRNAs (piR-hsa-2854993, piR-hsa-1250731 and

piR-hsa-1303866), which all were found in lower levels in the O-arm. In contrast, the remaining three sncRNAs (RNU2-4P, RNU2-59P, Hsa-Mir-202\_pri) were all found in higher levels in the O-arm. Hsa-Mir-202\_pri decreased significantly in the O-arm but did not change in the G-arm. Even though the two arms were not tested directly against each other, the differences in longitudinal expression patterns could indicate that subcapsular orchectomy clears piRNAs from circulation more efficiently or faster compared with GnRH-agonist treatment.

[Figure 5]



## Discussion

Here we report changes in the level of circulating sncRNAs in a cohort of 57 patients with prostate cancer who were treated with either subcapsular orchectomy or GnRH-agonist. In both treatment arms, significantly altered sncRNAs were mostly found in lower levels after the intervention, indicating a pronounced loss of sncRNAs after castration. The majority of the sncRNAs that changed were piRNAs, which are largely specific to the testis in non-pathological conditions, and hence fit with a removal of testicular function. However, even though the levels of most piRNAs dropped post-intervention, piRNAs were still

detectable and some even increased. Because piRNAs are nearly unique to germ cells [45], we had expected that post-intervention levels should be close to zero - especially in the O-arm where all germ cells are surgically removed. However, piRNAs have also been reported to be aberrantly expressed in different types of cancers [46, 47] including prostate cancer [46]. Indeed, one of the two piRNAs that were consistently upregulated post-intervention, piR-hsa-82907, is reported to target *SNHG1* in prostate cancer tissue and is associated with an unfavourable prognosis [48]. Hence, it is possible that some piRNAs in circulation originate from the cancer in the prostate of these patients. The circulating half-life of piRNAs, and sncRNAs in general, is not well-described and could also contribute to the detection of piRNAs - even months after orchiectomy. Lastly, due to a rather poor annotation of piRNAs in combination with their short sequence length, some tRNA fragments can incorrectly be annotated as piRNAs [49]. To minimise this risk we checked that none of the piRNAs that we found differentially expressed have been listed as ambiguously annotated in humans [47, 49], which none were, and in our annotation pipeline reads were, in addition, also mapped to tRNAs before piRNAs, which minimises the risk of incorrect annotation.

Interestingly, we found that seven of the differentially present piRNAs, which were significantly downregulated in both the O- and G-arm, had *HSPA9* as a possible target. *HSPA9* has been linked to the aggressiveness of prostate cancer [50] and we speculate whether the decreasing levels of these circulating piRNAs could be related to the response of the cancer to the two modes of castration. Four of the piRNAs also had *SNORD63* as a possible target but it is unknown whether *SNORD63* also could be related to prostate cancer or the testis but it has been suggested as a biomarker for clear cell renal carcinoma in urine [51]. In general, we still lack knowledge about the potential function of piRNAs outside germ cells and this hence remains quite speculative.

Much more information is available on miRNAs, and the miRNAs found to be altered in this study have all been related to prostate cancer before. We found that both precursors of miR-153, mir-153-1-pri (chromosome 2) and miR-153-2-pri (chromosome 7), were significantly downregulated after treatment in both arms. The mature miRNA, miR-153, has been reported to be upregulated in prostate cancer tissue [52] and has oncogenic potential by downregulating PTEN, which in turn acts as a suppressor of the PI3K/Akt pathway [53]. Thus, the decrease in the circulating levels of the miR-153 precursors could reflect the treatment of the prostate cancer rather than being an effect of castration. However, miR-153 has also been reported in extracellular vesicles from semen and has a higher expression in the testis compared to prostate (and epididymis) [54], which corroborates our findings by RT-qPCR. The decrease in the miR-153 precursor levels could hence also be due to the lack of contribution to the seminal fluid from the testicles or the combination of this and the prostate cancer treatment. Similarly, both miR-184 and miR-96 have been reported in relation to prostate cancer. miR-184 decreased post-intervention in the O-arm and is a potential suppressor of tumorigenesis in prostate cancer [55]. miR-96 decreased in the G-arm and this miRNA has previously been shown to be a regulator of the androgen receptor and to drive tumour progression in prostate cancer [56]. Together, these findings indicate that some of the changes in circulating sncRNAs, i.e. the decrease in these miRNAs, potentially can be attributed to the presence of cancer in the prostate and the treatment response, whereas others are directly related to the removal of the testis. In other words, tumour dynamics and the loss of testicular function or testicular tissue could all influence the circulating sncRNAs and this study is not able to disentangle one source from the other.

For the snoRNAs and snRNAs, specific functional information is sparse. RNU5B-1 is part of the U5 small nuclear ribonucleoprotein complex involved in splicing of

mRNAs. Although mRNA splicing is a general cellular function needed in all cell types, RNU5B-1 has a unique and high expression in the testis (GTEx [44]). *In situ* hybridization results showed SNORD38A to have a high expression primarily in spermatogonia. SNORD38A is involved in the 2'-O-methylation of rRNA, a function needed in all cell types, and was identified as a potential part of the aetiology behind Alzheimer's disease in a mouse model [57]. However, much still remains to be discovered about the potential function of the identified snRNAs and snoRNAs.

The two different treatment arms represent two very different types of castration, and this was also reflected in the sncRNA profile. Triptorelin, the GnRH-agonist used in the G-arm, is superior in terms of reduction of testosterone levels [27] and the metabolic consequences of the two treatments also differ [29]. Specifically for this cohort, it was previously shown that both treatments resulted in adverse changes in parameters such as body composition, serum cholesterols, and increased insulin resistance already at week 12 and 24. Furthermore, the authors also found a larger increase in fat mass in the G-arm [29]. Therefore, some of the detected differences between the two treatment arms could also be driven by metabolic differences. Furthermore, in the G-arm, patients were also treated with the antiandrogen Bicalutamide (50 mg daily for the first 30 days), as an anti-flare precaution [27], and this could also lead to differences in the sncRNA profile. We investigated whether the level of sncRNAs could be directly associated with changes in testosterone levels but found no such association when the two arms were analysed together (data not shown). This might reflect that Triptorelin targets the HPG axis in contrast to the subcapsular orchiectomy. This is supported by the fact that three of the six sncRNAs consistently altered between the two treatment arms were piRNAs, which all decreased in the O-arm (testicular origin) and likely

reflect the difference between having the testicles removed (O-arm) versus targeting the HPG axis (G-arm).

We have already mentioned some limitations of our study, but other limitations include the likely decreased testicular function among men at the age of around 70 years. This would imply that circulating sncRNAs at baseline may not represent secretion from a testis with complete and ongoing spermatogenesis. Also, the long storage time may have affected the samples. However, such an effect would have impacted baseline and post-treatment samples equally and hence have little effect on which sncRNAs we identified as differentially present.

Strengths include the randomised design of the original study and the possibility of paired setup for this study. Furthermore, we sequenced our samples quite deep (average 10M mapped reads), which increases our sensitivity to detect changes in sncRNA levels.

In conclusion, our study reveals that several sncRNAs are significantly altered in circulation after castration and shows a substantial loss of piRNAs, likely having a testicular origin. However, more research is needed to confirm our findings and to deduce whether the identified sncRNAs carry endocrine information.

## Data availability

The small RNA sequencing data in this study have been deposited in the European Nucleotide Archive (ENA; <https://www.ebi.ac.uk/ena/>) at EMBL-EBI under accession number PRJEB106978.

# References

## References

1. Quinn, J.J. and H.Y. Chang, *Unique features of long non-coding RNA biogenesis and function*. Nat Rev Genet, 2016. **17**(1): p. 47-62.
2. Ha, M. and V.N. Kim, *Regulation of microRNA biogenesis*. Nat Rev Mol Cell Biol, 2014. **15**(8): p. 509-24.
3. Vasudevan, S., *Posttranscriptional upregulation by microRNAs*. Wiley Interdiscip Rev RNA, 2012. **3**(3): p. 311-30.
4. Makarova, J.A., et al., *Intracellular and extracellular microRNA: An update on localization and biological role*. Prog Histochem Cytochem, 2016. **51**(3-4): p. 33-49.
5. Nagirnaja, L., et al., *Diverse monogenic subforms of human spermatogenic failure*. Nat Commun, 2022. **13**(1): p. 7953.
6. Nagirnaja, L., et al., *Variant PNLDC1, Defective piRNA Processing, and Azoospermia*. N Engl J Med, 2021. **385**(8): p. 707-719.
7. Birgit Stallmeyer, C.B., Rytis Stakaitis et al.m, *Inherited defects of piRNA biogenesis cause transposon de-repression, impaired spermatogenesis, and human male infertility*. 2024.
8. O'Brien, J., et al., *Overview of MicroRNA Biogenesis, Mechanisms of Actions, and Circulation*. Front Endocrinol (Lausanne), 2018. **9**: p. 402.
9. Bayraktar, R., K. Van Roosbroeck, and G.A. Calin, *Cell-to-cell communication: microRNAs as hormones*. Mol Oncol, 2017. **11**(12): p. 1673-1686.
10. Kosaka, N., et al., *Secretory mechanisms and intercellular transfer of microRNAs in living cells*. J Biol Chem, 2010. **285**(23): p. 17442-52.
11. Zhang, Y., et al., *Secreted monocytic miR-150 enhances targeted endothelial cell migration*. Mol Cell, 2010. **39**(1): p. 133-44.
12. Pardini, B., et al., *Noncoding RNAs in Extracellular Fluids as Cancer Biomarkers: The New Frontier of Liquid Biopsies*. Cancers (Basel), 2019. **11**(8).
13. Collino, F., et al., *Microvesicles derived from adult human bone marrow and tissue specific mesenchymal stem cells shuttle selected pattern of miRNAs*. PLoS One, 2010. **5**(7): p. e11803.
14. Florijn, B.W., et al., *Diabetic Nephropathy Alters the Distribution of Circulating Angiogenic MicroRNAs Among Extracellular Vesicles, HDL, and Ago-2*. Diabetes, 2019. **68**(12): p. 2287-2300.
15. Arroyo, J.D., et al., *Argonaute2 complexes carry a population of circulating microRNAs independent of vesicles in human plasma*. Proc Natl Acad Sci U S A, 2011. **108**(12): p. 5003-8.
16. Fabbri, M., *MicroRNAs and miRceptors: a new mechanism of action for intercellular communication*. Philos Trans R Soc Lond B Biol Sci, 2018. **373**(1737).
17. Almstrup, K., et al., *Application of miRNAs in the diagnosis and monitoring of testicular germ cell tumours*. Nat Rev Urol, 2020. **17**(4): p. 201-213.
18. Pinchi, E., et al., *miR-1, miR-499 and miR-208 are sensitive markers to diagnose sudden death due to early acute myocardial infarction*. J Cell Mol Med, 2019. **23**(9): p. 6005-6016.
19. Angelescu, M.A., et al., *miRNAs as Biomarkers in Diabetes: Moving towards Precision Medicine*. Int J Mol Sci, 2022. **23**(21).

20. Messina, A., et al., *A microRNA switch regulates the rise in hypothalamic GnRH production before puberty*. Nat Neurosci, 2016. **19**(6): p. 835-44.
21. Heras, V., et al., *Hypothalamic miR-30 regulates puberty onset via repression of the puberty-suppressing factor, Mkrn3*. PLoS Biol, 2019. **17**(11): p. e3000532.
22. Varimo, T., et al., *Circulating miR-30b levels increase during male puberty*. Eur J Endocrinol, 2021. **184**(5): p. K11-k14.
23. Mørup, N., et al., *Circulating levels and the bioactivity of miR-30b increase during pubertal progression in boys*. Front Endocrinol (Lausanne), 2023. **14**: p. 1120115.
24. Rodie, M.E., et al., *Androgen-responsive non-coding small RNAs extend the potential of HCG stimulation to act as a bioassay of androgen sufficiency*. Eur J Endocrinol, 2017. **177**(4): p. 339-346.
25. Kangas, R., et al., *Circulating miR-21, miR-146a and Fas ligand respond to postmenopausal estrogen-based hormone replacement therapy--a study with monozygotic twin pairs*. Mech Ageing Dev, 2014. **143-144**: p. 1-8.
26. Kangas, R., et al., *Aging and serum exomiR content in women--effects of estrogenic hormone replacement therapy*. Sci Rep, 2017. **7**: p. 42702.
27. Østergren, P.B., et al., *Luteinizing Hormone-Releasing Hormone Agonists are Superior to Subcapsular Orchiectomy in Lowering Testosterone Levels of Men with Prostate Cancer: Results from a Randomized Clinical Trial*. J Urol, 2017. **197**(6): p. 1441-1447.
28. Oken, M.M., et al., *Toxicity and response criteria of the Eastern Cooperative Oncology Group*. Am J Clin Oncol, 1982. **5**(6): p. 649-55.
29. Østergren, P.B., et al., *Metabolic consequences of gonadotropin-releasing hormone agonists vs orchiectomy: a randomized clinical study*. BJU Int, 2019. **123**(4): p. 602-611.
30. Albrethsen, J., et al., *Serum Insulin-like Factor 3, Testosterone, and LH in Experimental and Therapeutic Testicular Suppression*. J Clin Endocrinol Metab, 2023. **108**(11): p. 2834-2839.
31. Dissing, N., et al., *Changes in Quality of Life and Sexual Function After Luteinizing Hormone-Releasing Hormone (LHRH) Agonists and Orchiectomy in Men With Metastatic Prostate Cancer: Results From a Randomized Trial*. Cureus, 2024. **16**(3): p. e55934.
32. Martin, M., *Cutadapt removes adapter sequences from high-throughput sequencing reads*. EMBnet.journal, [S.I.], v. 17, n. 1, p. pp. 10-12, may 2011. ISSN 2226-6089. doi:<https://doi.org/10.14806/ej.17.1.200>.
33. Langmead B, T.C., Pop M, Salzberg SL, *Ultrafast and memory-efficient alignment of short DNA sequences to the human genome*. Genome Biol 10:R25.
34. Robinson, M.D., D.J. McCarthy, and G.K. Smyth, *edgeR: a Bioconductor package for differential expression analysis of digital gene expression data*. Bioinformatics, 2010. **26**(1): p. 139-40.
35. Blighe K, R.S., Lewis M *EnhancedVolcano: Publication-ready volcano plots with enhanced colouring and labeling*. 2024(R package version 1.22.0,).
36. Wickam, H., *ggplot2: Elegant Graphics for Data Analysis*. 2016, Springer-Verlag New York.
37. Kassambara, A., *ggpubr: 'ggplot2' Based Publication Ready Plots*. 2023.
38. Dyer, S.C., et al., *Ensembl 2025*. Nucleic Acids Research, 2024. **53**(D1): p. D948-D957.
39. Center for Big Data Research in Health, K.L.o.R.B., Institute of Biophysics, Chinese Academy of Sciences, *piRBase*. 2025.
40. *miRNATissueAtlas 2025*. 2025, Chair for Clinical Bioinformatics, Saarland University.

41. Wang, W.L.X., *Prediction of functional microRNA targets by integrative modeling of microRNA binding and target expression data*. *Genome Biology*, 2019. **20(1):18**.
42. Wang, Y.C.X., *miRDB: an online database for prediction of functional microRNA targets*. *Nucleic Acids Research*, 2020. **48(D1):D127-D131**.
43. Bergeron D, P.H., Fafard-Couture É, Deschamps-Francoeur G, Faucher-Giguère L, Bouchard-Bourelle P, Abou Elela S, Catez F, Marcel V, Scott MS, *snoDB 2.0: an enhanced interactive database, specializing in human snoRNAs*. *Nucleic Acids Research*, 2023. **51(D1):D291-D296**.
44. *GTEX*.
45. Girard, A., et al., *A germline-specific class of small RNAs binds mammalian Piwi proteins*. *Nature*, 2006. **442**(7099): p. 199-202.
46. Zhang, L., et al., *piR-31470 epigenetically suppresses the expression of glutathione S-transferase pi 1 in prostate cancer via DNA methylation*. *Cellular Signalling*, 2020. **67**: p. 109501.
47. Saritas, G., et al., *PIWI-interacting RNAs and human testicular function*. *WIREs Mech Dis*, 2022. **14**(6): p. e1572.
48. Xie, M., Z. Zhang, and Y. Cui, *Long Noncoding RNA SNHG1 Contributes to the Promotion of Prostate Cancer Cells Through Regulating miR-377-3p/AKT2 Axis*. *Cancer Biother Radiopharm*, 2020. **35**(2): p. 109-119.
49. Tosar, J.P., C. Rovira, and A. Cayota, *Non-coding RNA fragments account for the majority of annotated piRNAs expressed in somatic non-gonadal tissues*. *Communications Biology*, 2018. **1**(1): p. 2.
50. Shipitsin, M., et al., *Identification of proteomic biomarkers predicting prostate cancer aggressiveness and lethality despite biopsy-sampling error*. *Br J Cancer*, 2014. **111**(6): p. 1201-12.
51. Shang, X., et al., *SNORD63 and SNORD96A as the non-invasive diagnostic biomarkers for clear cell renal cell carcinoma*. *Cancer Cell Int*, 2021. **21**(1): p. 56.
52. Gilyazova, I., et al., *The potential of miR-153 as aggressive prostate cancer biomarker*. *Noncoding RNA Res*, 2023. **8**(1): p. 53-59.
53. Yousefnia, S., *A comprehensive review on miR-153: Mechanistic and controversial roles of miR-153 in tumorigenicity of cancer cells*. *Front Oncol*, 2022. **12**: p. 985897.
54. Larriba, S., et al., *Seminal extracellular vesicle sncRNA sequencing reveals altered miRNA/isomiR profiles as sperm retrieval biomarkers for azoospermia*. *Andrology*, 2024. **12**(1): p. 137-156.
55. Tan, G.G., et al., *miR-184 delays cell proliferation, migration and invasion in prostate cancer by directly suppressing DLX1*. *Exp Ther Med*, 2021. **22**(4): p. 1163.
56. Long, M.D., et al., *The miR-96 and RAR $\gamma$  signaling axis governs androgen signaling and prostate cancer progression*. *Oncogene*, 2019. **38**(3): p. 421-444.
57. Lio, C.T., et al., *Small RNA Sequencing in the Tg4-42 Mouse Model Suggests the Involvement of snoRNAs in the Etiology of Alzheimer's Disease*. *J Alzheimers Dis*, 2022. **87**(4): p. 1671-1681.

## Author contribution statement

KA, NM and AMM designed the study. AMM, KA and NM collected, analysed and interpreted the data. LS and SW did qPCR and *in situ* hybridization. AMM, KA, LS, and SW wrote the manuscript. PØ, MF, JS and AJ provided materials for analysis and specialist knowledge. All authors contributed to the final editing of the manuscript.

## Additional information

**Funding declaration:** Novo Nordisk Foundation (grant numbers NNF210C0069913 and NNF21C0069969 to KA), the Svend Andersen Foundation, and the Independent Research Fund (grant number: 1030-0381B to KA).

**Disclosure summary:** MF has been speaker and advisory board member of Astellas Pharma. All other authors have nothing to disclose.

## Figure legends

**Figure 1: Overview of study cohort.** Men with prostate cancer (n=57) were randomised to castration either by medical treatment with the GnRH-agonist, Triptorelin (G-arm) or by subcapsular orchiectomy (O-arm). Blood samples were taken before intervention (week 0; W0) and at week 12 (W12) and 24 (W24). Created in BioRender. Almstrup, K. (2025) <https://BioRender.com/zdwl3je>

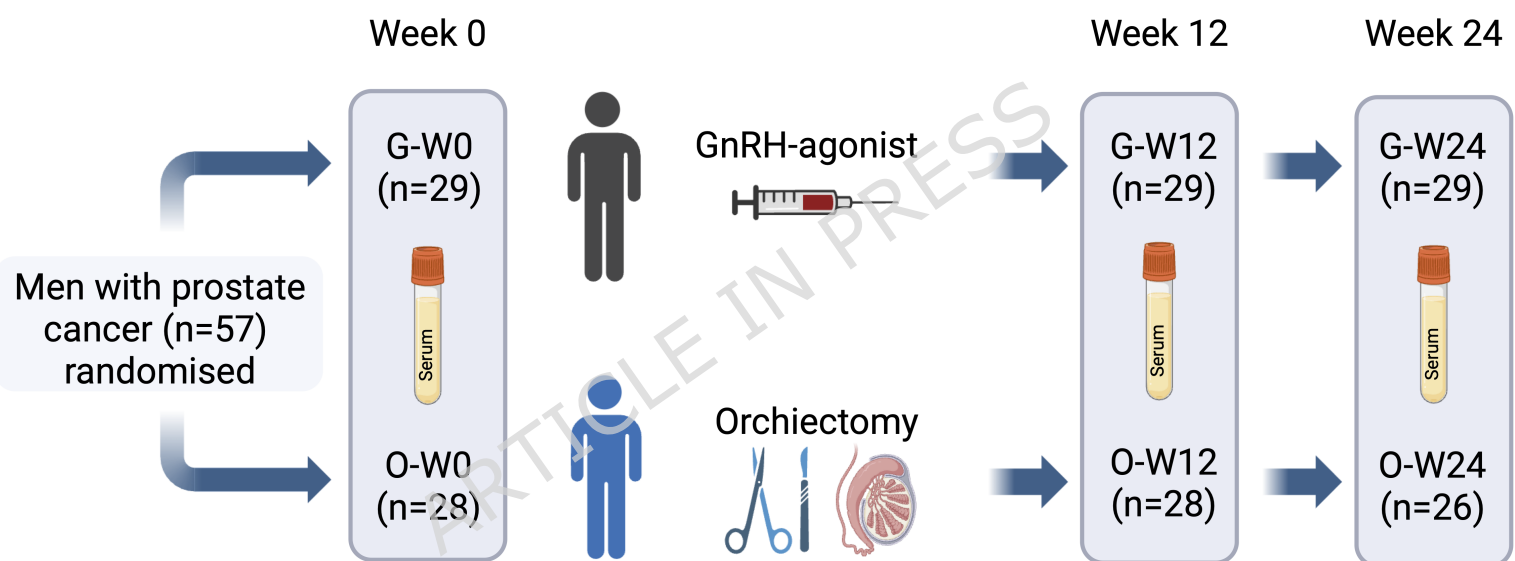
**Figure 2: Identification of differentially expressed sncRNAs in the two treatment arms.** Generalised linear models identified sncRNAs present in significantly altered levels at W12 and W24 in contrast to W0. The analyses are based on the following distribution of samples across the three timepoints: O-arm W0 (n=27), W12 (n=28), and W24 (n=24) and G-arm W0 (n=29), W12 (n=29), and W24 (n=26). In **a**, volcano plots illustrate the sncRNAs that are significant at FDR q-value <0.05 and regulated more than 1-fold (red dots). Blue and green dots mark sncRNAs that are <1 fold regulated and have q-values >0.05, respectively. The dotted lines indicate an FDR q-value of 0.05 and a fold change of 1. The name is displayed for the 10 most significant sncRNAs in each contrast. Top row from the left: differentially expressed sncRNA in the group of patients that had subcapsular orchiectomies (O-arm) for contrasts W12, W24, and W12 + W24 in reference to W0. The bottom row shows the same for the group of patients receiving GnRH-agonist (G-arm). In **b**, the number of sncRNAs identified at FDR q-value <0.05 in each contrast, is plotted according to the subtype (miRNAs, piRNAs, pre-miRNAs, snoRNAs, snRNAs, and tRNAs). The plots on top shows the number of sncRNAs identified in higher levels post-intervention (i.e. at W12 and W24) and the plots below shows sncRNAs identified in lower levels after intervention.

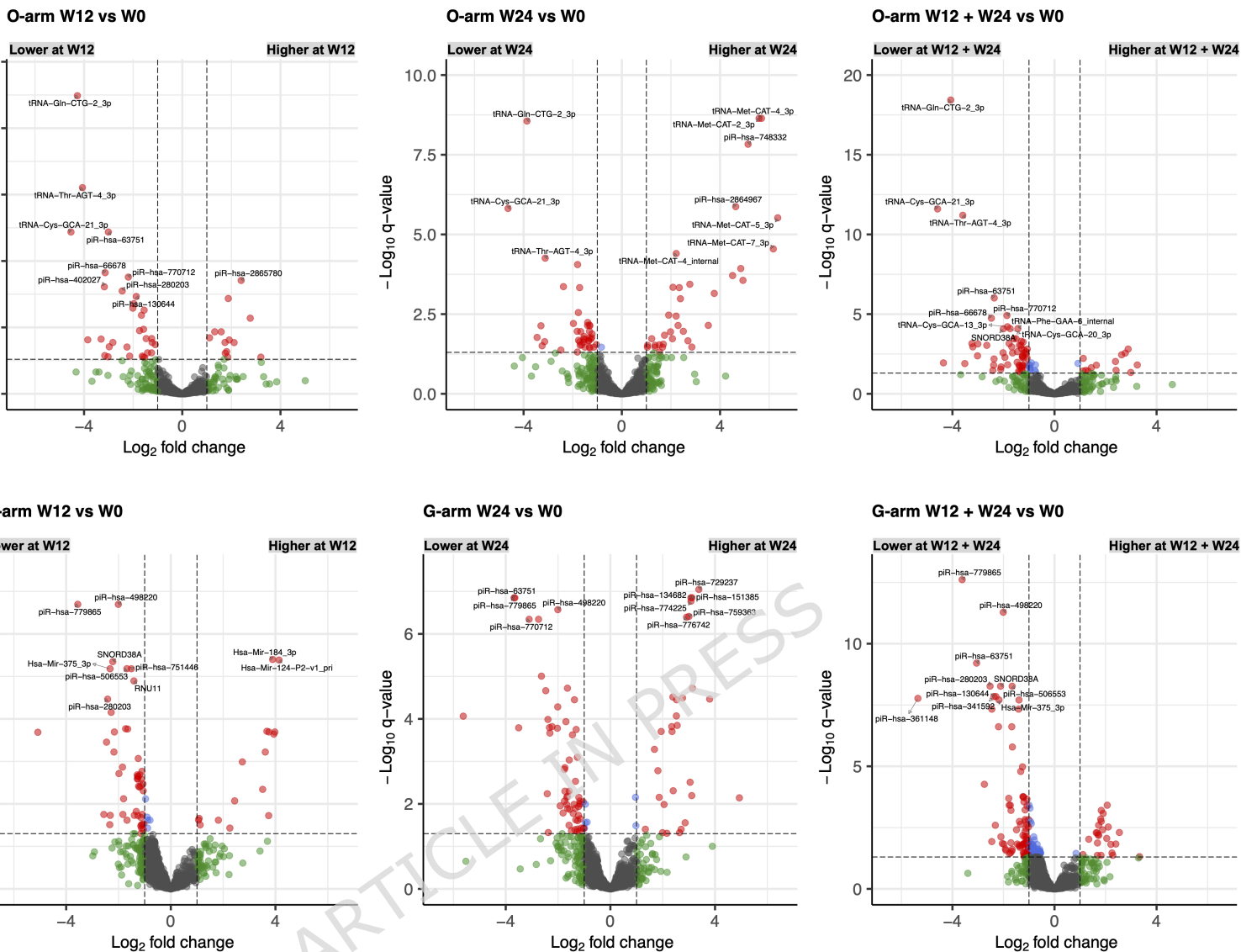
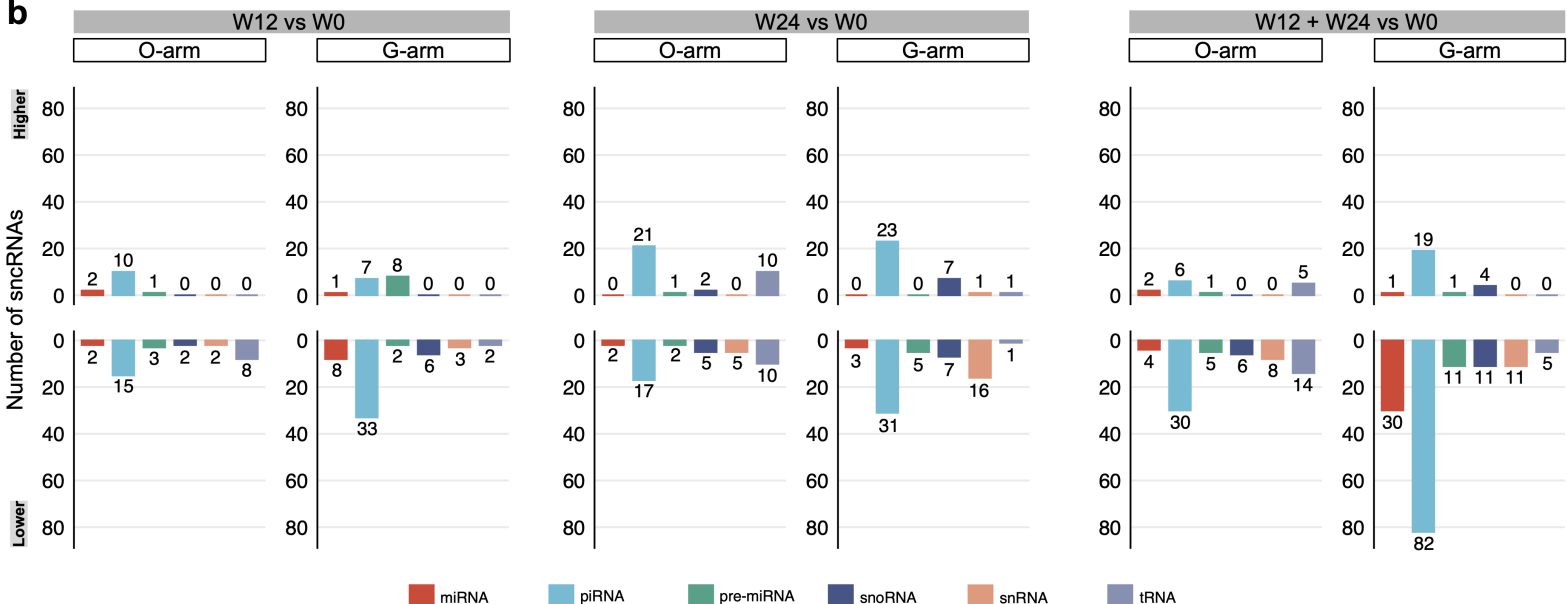
**Figure 3: Venn diagram showing overlapping and exclusive sncRNAs in different comparative groups.** In **a** and **b**, the Venn diagram outlines the number of significantly different sncRNAs between the three different analysis contrasts for the O-arm and the G-arm, respectively. In **c**, the Venn diagram shows the overlap between significant sncRNAs identified at W24 vs W0 as well as W12 + W24 vs W0 for both the O-arm and the G-arm.

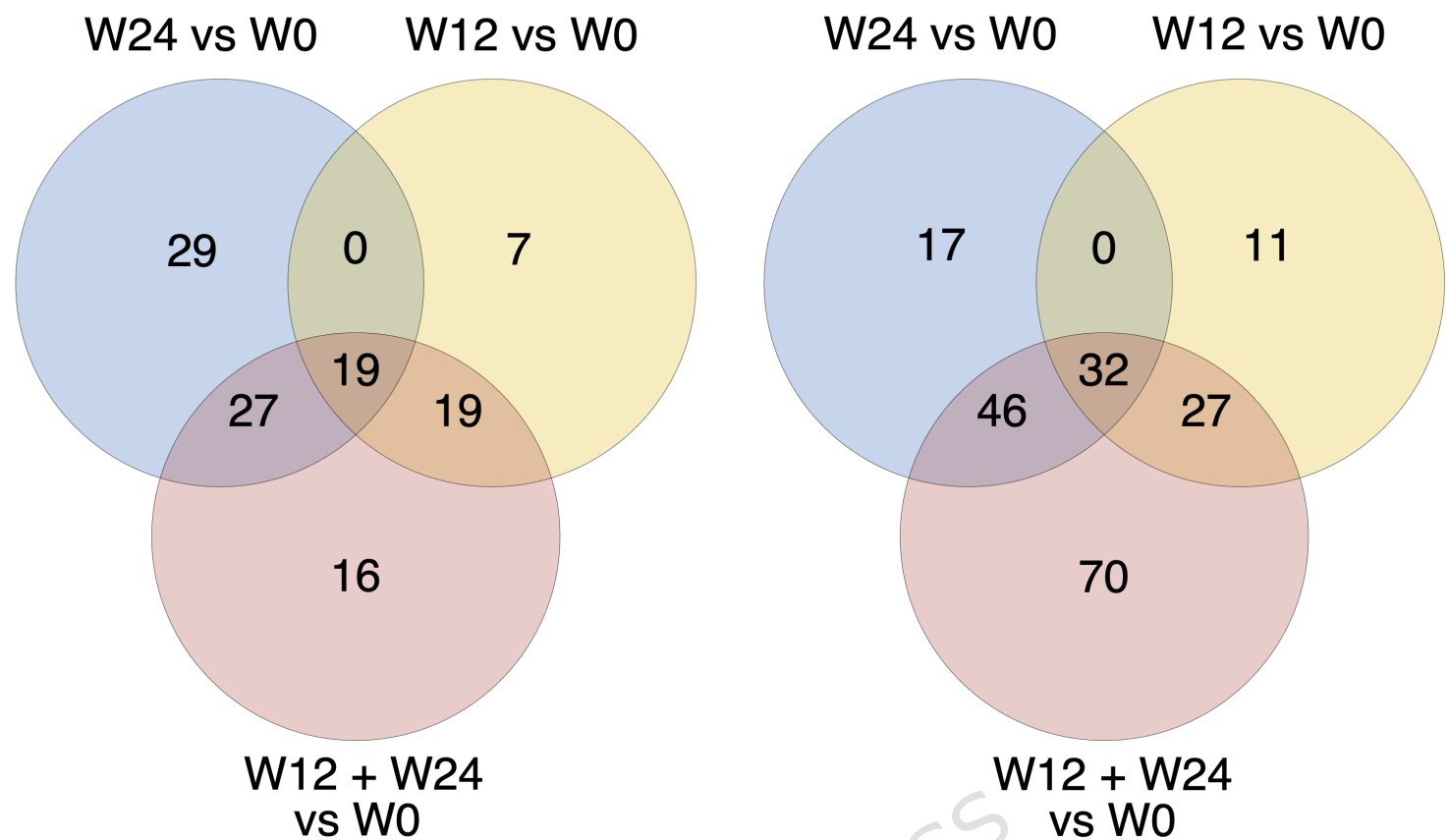
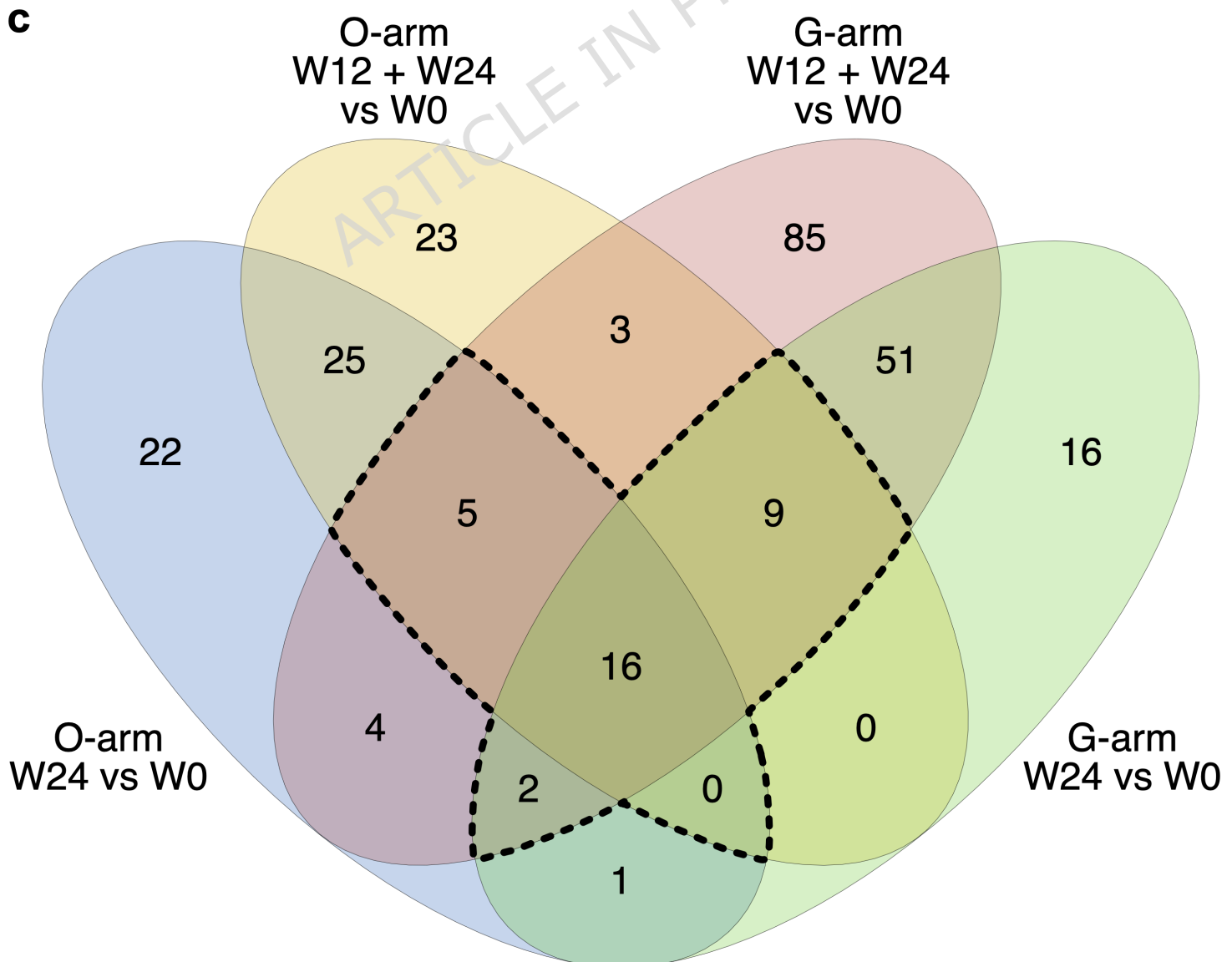
**Figure 4: Longitudinal expression patterns and experimental validation of testicular expression of selected sncRNAs.** Subpanels **a-f** show longitudinal traces of six sncRNAs for both the O and G-arm. Boxplots are shown for each timepoint (W0, W12 and W24) and treatment arm, and on top of the boxplot, points representing each participant are shown and connected with a line. Within each treatment arm, the colours represent a single participant. In **g** and **f**, results from RT-qPCR quantification of expression in the testis, skin, prostate, and epididymis are shown for miR-153-P1\_pri and *SNORD38A*. The relative expression levels in six different commercially available RNA samples are shown. Expression was normalized to the housekeeping gene ACTB. Error bars are based on biological replicates for testis tissue (n=3). Error bars for skin, prostate, and epididymis are based on technical variability (1 sample, 3 technical replicates for each). In **i**, small RNA *in situ* hybridisation of *SNORD38A* in testis tissue samples from tumour-free periphery of orchietomy specimens from two adult men with testicular germ cell tumours show a prominent expression in spermatogonia (arrows) and some expression in Leydig (arrow heads) and peritubular cells. The dashed box indicates the magnified area shown below. The bar indicates 50 and 20  $\mu$ m, respectively.

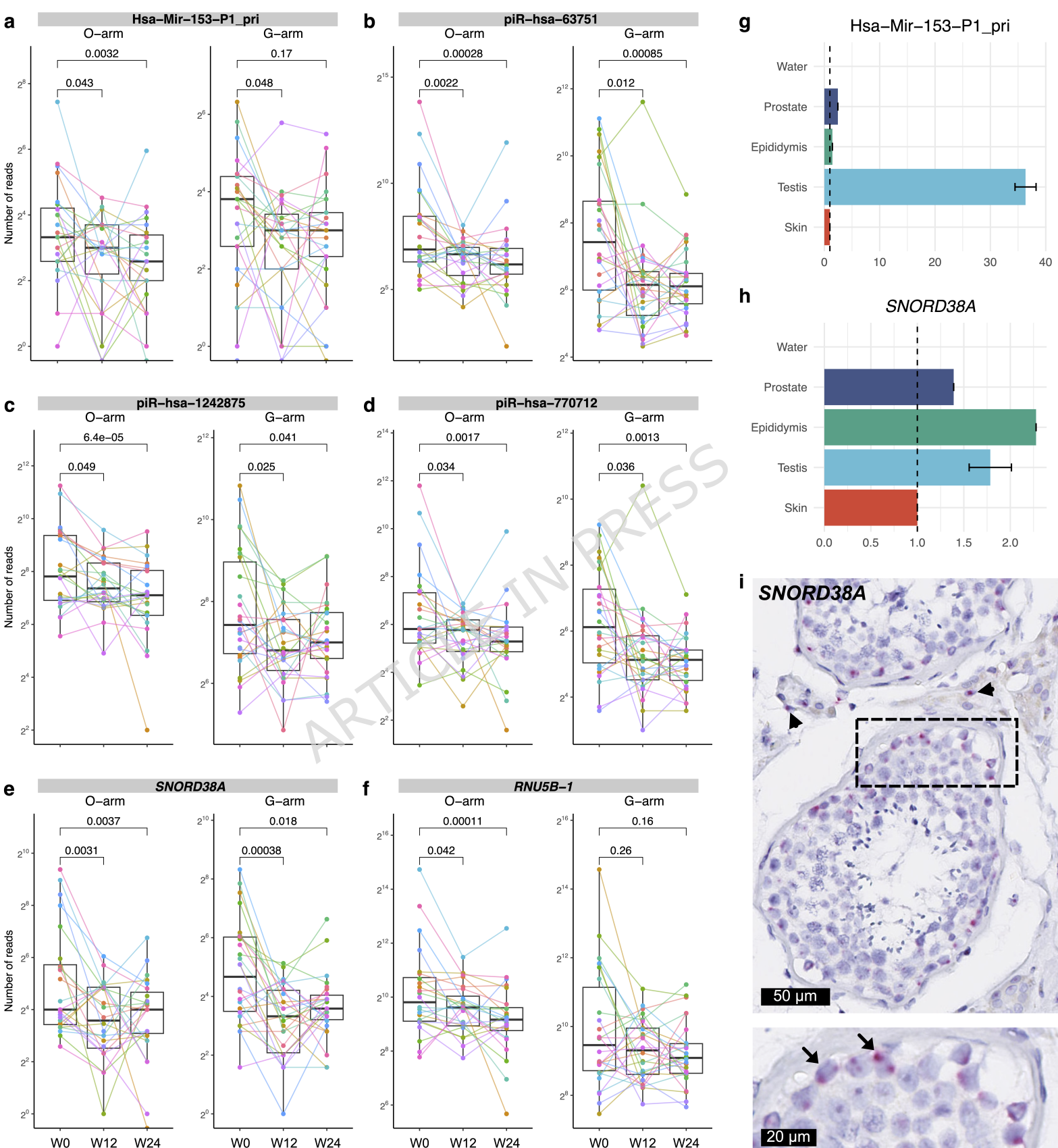
**Figure 5: Differences in circulating sncRNAs between the two types of intervention.** Volcano plots showing sncRNAs differentially present at W12 (left)

and at W24 (right) and a Venn diagram depicting the overlap between the two post-intervention time points in the middle. The six sncRNAs that overlap at both W12 and W24 are outlined below the Venn diagram and the arrow indicate the direction relative to the G-arm (i.e., arrow down imply downregulation in O-arm relative to G-arm).

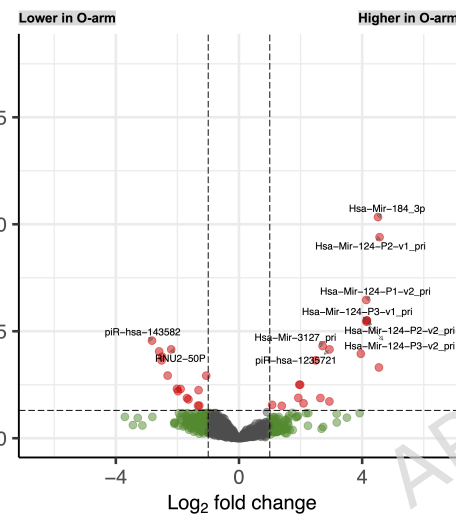


**a****b**

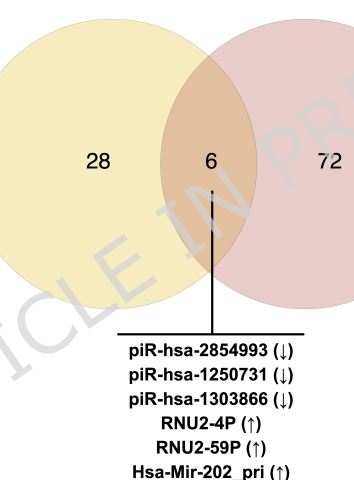
**a****c**



## W12 O- vs G-arm



## W12 O- vs G-arm



## W24 O- vs G-arm

## W24 O- vs G-arm

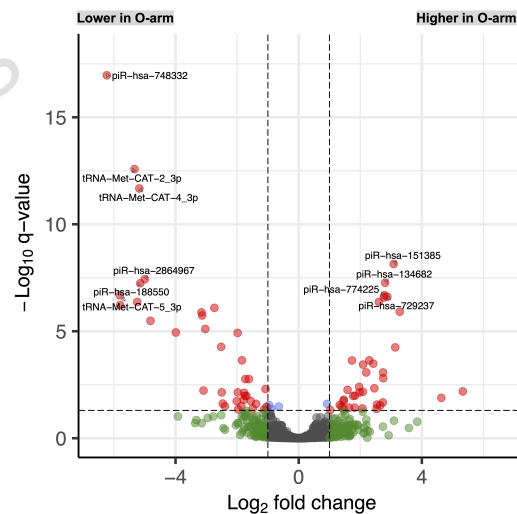


**Table 1: Study population characteristics at baseline.** BMI = Body Mass Index, ECOG = Eastern Cooperative Oncology Group (ECOG) Performance Status Scale. Values are mean (SD) for age, BMI, and testosterone levels. ECOG values are n (%).

	O-arm	G-arm	p-value
<b>Individuals (n)</b>	28	29	-
<b>Treatment</b>	Subcapsular orchectomy	GnRH-analogue (Triptorelin)	
<b>Age</b>	72.1 (8.8)	74.8 (5.8)	0.18
<b>BMI</b>	27.0 (4.8)	27.6 (3.5)	0.60
<b>Testosterone (nmol/L)</b>	15.1 (6.5)	13.0 (6.3)	0.23
<b>ECOG n (%)</b>			
0	16 (57)	20 (69)	-
1	11 (39)	7 (24)	-
2	1 (4)	2 (7)	-

**Table 2: Information on the 32 differentially expressed sncRNAs (dashed lines in Figure 3c).** The information in the table was obtained from various databases as listed in the Methods and Materials section.

	O-arm logFC (FDR)	G-arm logFC (FDR)	piRNAs		miRNAs, snRNAs and snoRNAs		Potential target genes
			Testis RNAseq reads	Reported in germ cells	Expression in testis and prostate	Expression in testis and prostate	
<b>Intersecting all 4 group</b>							
piR-hsa-2864967	2.77 (0.0028)	1.71 (0.0132)	Yes	Yes	-	-	
piR-hsa-770712	-1.87 (1.2*10^-5)	-2.46 (4.7*10^-8)	Yes	Yes	-	-	PLEKHA8P1, ENSG00000286171
piR-hsa-66678	-2.48 (1.8 *10^-5)	-2.75 (5.4*10^-5)	Yes	Yes	-	-	THAP8
piR-hsa-63751	-2.36 (9.7*10^-7)	-3.05 (6.2*10^-10)	Yes	Yes	-	-	THAP8
piR-hsa-741466	-1.19 (0.0018)	-1.2 (0.0003)	No	Yes	-	-	HSPA9, SNORD63
piR-hsa-1242875	-1.13 0.0023)	-1.24 (0.0002)	No	Yes	-	-	HSPA9, SNORD63
piR-hsa-1288242	-1.11 (0.0032)	-1.22 (0.0002)	No	Yes	-	-	HSPA9, SNORD63
piR-hsa-1254147	-0.96 (0.024)	-1.12 (0.0034)	No	Yes	-	-	HSPA9, SNORD63
Hsa-Mir-153-P2-pri	-1.68 (0.0011)	-1.28 (0.0075)	-	-	Testis and prostate	UNC5C, KCNQ4, SERTAD2, KLF5, HEY2	
Hsa-Mir-153-P1-pri	-1.78 (0.0007)	-1.19 (0.0077)	-	-	Testis and prostate	UNC5C, KCNQ4, SERTAD2, KLF5, HEY2	
tRNA-Gln-CTG-2_3p	-4.07 (3.7*10^-19)	-0.82 (0.023)	-	-	-	-	
RNU5B-1	-1.23 (0.00057)	-1.67 (2.4*10^-7)	-	-	Highest median expression in testis	-	
RNU11	-1.07 (0.0016)	-1.39 (2.0*10^-8)	-	-	-	-	
SNORD38A	-2 (8.3*10^-5)	-2.12 (5.4*10^-9)	-	-	Testis	-	
SNORD26	-1.29 (0.0015)	-1.14 (0.0017)	-	-	Testis	-	
SNORA2C	-1.07 (0.0059)	-1.22 (0.0002)	-	-	Testis	-	
<b>Intersecting 3 out of 4 groups</b>							
piR-hsa-130644	-1.51 (0.00035)	-2.3 (1.4*10^-8)	Yes	Yes	-	ENSG00000286171	
piR-hsa-774082	-1.37 (0.00091)	-1.71 (0.0006)	Yes	Yes	-	PLEKHA8P1, ENSG00000286171	
piR-hsa-368867	-1.24 (0.0044)	-1.79 (0.0002)	Yes	Yes	-	PLEKHA8P1, ENSG00000286171	
piR-hsa-102217	-1.95 (0.0052)	-2.05 (0.014)	Yes	Yes	-	-	
piR-hsa-147022	-1.21 (0.0058)	-1.73 (0.0004)	Yes	Yes	-	PLEKHA8P1, ENSG00000286171	
piR-hsa-280203	-1.46 (0.0105)	-2.53 (5.4*10^-9)	Yes	Yes	-	-	
piR-hsa-167536	-0.91(0.0114)	-1.06 (0.039)	Yes	Yes	-	PLEKHA8P1, ENSG00000286171	
SNORD14D	-1.39 (0.017)	-1.39 (0.017)	-	-	Testis	-	

piR-hsa-762831	-1.26 (0.035)	1.7 (0.0061)	Yes	Yes	-	-
piR-hsa-1301393	-1.18 (0.0027)	-0.98 (0.012)	No	Yes	-	HSPA9, SNORD63
piR-hsa-736316	-1.09 (0.016)	-1.03 (0.024)	No	Yes	-	HSPA9, SNORD63
piR-hsa-777409	-0.94 (0.028)	-0.99 (0.015)	No	Yes	-	HSPA9, SNORD63
Hsa-Mir-184_3p	-1.25 (0.0042)	1.68 (0.043)	-	-	Testis and prostate	SETD9, NUS1, CES2, PLPP3, GNB1
tRNA-Thr-AGT-4_3p	3.59 (6.3*10^-12)	-0.98 (0.034)	-	-	-	-
piR-hsa-82907	2.50 (0.0109) (W24)	2.05 (0.0087)	No	Yes	-	SNHG1
Hsa-Mir-96-P2_pri	2.39 (0.001) (W24)	-1.15 (0.0015)	-	-	Testis and prostate	NEXMIF, ADCY6, PRTG, SPIN1, FRS2

The information in the table was obtained from various databases as listed in the Methods and Materials section.